

Testing the Dark Matter Interpretation of the DAMA/LIBRA Result with Super-Kamiokande

Jonathan L. Feng

Department of Physics and Astronomy, University of California, Irvine, CA 92697,
USA

Jason Kumar

Department of Physics and Astronomy, University of California, Irvine, CA 92697,
USA

Department of Physics and Astronomy, University of Hawai'i, Honolulu, HI 96822,
USA

John Learned

Department of Physics and Astronomy, University of Hawai'i, Honolulu, HI 96822,
USA

Louis E. Strigari

Department of Physics and Astronomy, University of California, Irvine, CA 92697,
USA

Kavli Institute for Particle Astrophysics and Cosmology, Department of Physics,
Stanford University, Stanford, CA 94305, USA

Abstract. We consider the prospects for testing the dark matter interpretation of the DAMA/LIBRA signal with the Super-Kamiokande experiment. The DAMA/LIBRA signal favors dark matter with low mass and high scattering cross section. We show that these characteristics imply that the scattering cross section that enters the DAMA/LIBRA event rate determines the annihilation rate probed by Super-Kamiokande. Current limits from Super-Kamiokande through-going events do not test the DAMA/LIBRA favored region. We show, however, that upcoming analyses including fully-contained events with sensitivity to dark matter masses from 5 to 10 GeV may corroborate the DAMA/LIBRA signal. We conclude by considering three specific dark matter candidates, neutralinos, WIMPless dark matter, and mirror dark matter, which illustrate the various model-dependent assumptions entering our analysis.

PACS numbers: 95.35.+d, 04.65.+e, 12.60.Jv

1. Introduction

The DAMA/LIBRA experiment has seen, with 8.2σ significance [1], an annual modulation [2] in the rate of scattering events, which could be consistent with dark matter-nucleon scattering. Much of the region of dark matter parameter space that is favored by DAMA is excluded by null results from other direct detection experiments, including CRESST [3], CDMS [4], XENON10 [5], TEXONO [6, 7], and CoGeNT [8]. On the other hand, astrophysical uncertainties [9, 10] and detector effects [11] act to open up regions that may simultaneously accommodate the results from DAMA and these other experiments. Following DAMA’s latest results, several recent studies [12, 13, 14, 15, 16] have studied the consistency of DAMA with other direct detection experiments, with varying assumptions and varying conclusions. What is clear, however, is that if DAMA is seeing dark matter, the preferred region of parameter space has dark matter mass in the range $m_X \sim 1 - 10$ GeV and spin-independent proton scattering cross section $\sigma_{\text{SI}} \sim 10^{-5} - 10^{-2}$ pb. Although neutralinos have been proposed as a possible explanation [19], such low masses and high cross sections are not typical of weakly-interacting massive particles (WIMPs), and alternative dark matter candidates have been suggested to explain the DAMA signal [20, 21, 22, 23, 12, 24, 25, 26].

The current state of affairs also makes it abundantly clear that data from complementary experiments is likely required to sort out the true nature of this result and is certainly required to establish definitively the detection of dark matter. Other direct detection experiments may play this role. In this paper, we note that corroborating evidence may come from a very different source, namely, from the indirect detection of dark matter at Super-Kamiokande (Super-K). In contrast to direct detection experiments, which rapidly lose sensitivity at low masses, given physical limitations on threshold energies, Super-K’s limits remain strong for low masses. Super-K is therefore poised as one of the most promising experiments to either corroborate or exclude many dark matter interpretations of the DAMA/LIBRA data.

In Sec. 2, we show that, with a few well-motivated theoretical assumptions, the DAMA and Super-K event rates may be related. Currently published Super-K results do not challenge the DAMA preferred region. In Sec. 3, however, we show that there is significant potential for Super-K to extend its reach to dark matter masses from 5 to 20 GeV and provide sensitivity that is competitive with, or possibly much better than, direct detection experiments. In Sec. 4, we apply our analysis to three specific dark matter candidates that have been proposed to explain DAMA: neutralinos [19], WIMPless dark matter [21, 12, 22], and mirror dark matter [23]. These candidates illustrate and clarify the assumptions entering the analysis. We present our conclusions in Sec. 5.

As this work was in preparation, a study appeared that also considered testing the dark matter interpretation of DAMA with data from Super-K [27]. That work focused primarily on a model-independent approach and present Super-K data, considering neutralinos briefly as a case example, whereas this work considers neutralino, WIMPless,

and mirror dark matter and emphasizes the much brighter prospects for future Super-K results.

2. Relating Super-Kamiokande to DAMA

Super-K may indirectly detect dark matter by finding evidence for dark matter annihilation in the Sun or Earth’s core to standard model (SM) particles that then decay to neutrinos. In the case of muon neutrinos, the essential idea is to use the observed rate of upward-going muon events at Super-K to place an upper bound on the annihilation rate of dark matter in the Sun or the Earth’s core. In the low-mass region of interest, the dominant contribution to neutrino production via dark matter annihilation is from the Sun [28], and we will focus on the Sun below, although the Earth may also provide an interesting signal.

The total annihilation rate is

$$\Gamma = \frac{1}{2} C \tanh^2[(aC)^{\frac{1}{2}}\tau] , \quad (1)$$

where C is the capture rate, $\tau \simeq 4.5$ Gyr is the age of the solar system, and $a = \langle\sigma v\rangle/(4\sqrt{2}V)$, with σ the total dark matter annihilation cross section and V the effective volume of WIMPs in the Sun ($V = 5.7 \times 10^{30} \text{ cm}^3 (1 \text{ GeV}/m_X)^{3/2}$ [28, 31, 27]). It has been shown [29, 28, 30] that if $\langle\sigma v\rangle \sim 10^{-26} \text{ cm}^3 \text{ s}^{-1}$, as required for the thermal relic density of dark matter to be in the observed range, then for the range of parameters used in this work the Sun is in equilibrium (with an equilibration time ~ 420 million years), and $\Gamma \approx \frac{1}{2}C$. The thermalization of captured dark matter in the core of the sun occurs much more rapidly [34, 35]. For the dark matter mass $\gtrsim 4 \text{ GeV}$, which we assume here, WIMP evaporation is not relevant [29, 31, 27].

The dark matter capture rate is [28]

$$C = \left[\left(\frac{8}{3\pi} \right)^{\frac{1}{2}} \sigma \frac{\rho_X}{m_X} \bar{v} \frac{M_B}{m} \right] \left[\frac{3}{2} \frac{\langle v^2 \rangle}{\bar{v}^2} \right] f_2 f_3 . \quad (2)$$

The first bracketed factor counts the rate of dark matter-nucleus interactions: σ is the dark matter-nucleus scattering cross section, ρ_X/m_X is the local dark matter number density, m is the mass of the nucleus, and M_B is the mass of the capturing object. The mean velocity of the dark matter is \bar{v} , and $\langle v^2 \rangle$ is the squared escape velocity averaged throughout the Sun. The second bracketed expression is the “focusing” factor that accounts for the likelihood that a scattering event will cause the dark matter particle to be captured. The parameters f_2 and f_3 are computable $\mathcal{O}(1)$ suppression factors that account for the motion of the Sun and the mismatch between X and nucleus masses, respectively. f_3 will be close to 1 for solar capture [28]. The point is that given astrophysical assumptions about the density and velocity distribution of dark matter, the capture rate is completely computable as a function of the ratio σ/m_X . Roughly, assuming $\rho_X = 0.3 \text{ GeV cm}^{-3}$, $\bar{v} \sim 300 \frac{\text{km}}{\text{s}}$, $\frac{3}{2} \frac{\langle v^2 \rangle}{\bar{v}^2} \sim 20$ [28], and taking $f_2 \sim f_3 \sim 1$, one finds $C \sim 10^{29} (\sigma/m_X) \text{ GeV pb}^{-1} \text{ s}^{-1}$.

The major remaining particle physics uncertainty is the neutrino spectrum that arises from dark matter annihilation. This information is encoded in the function [32]

$$\xi(m_X) = \sum_F B_F [3.47 \langle Nz^2 \rangle_{F,\nu} + 2.08 \langle Nz^2 \rangle_{F,\bar{\nu}}] , \quad (3)$$

which relates the dark matter annihilation rate to the rate of muon events at a detector. The B_F are the branching fractions to each of the F SM final states summed over, and the $\langle Nz^2 \rangle$ are the second moments of the (anti-)neutrino energy spectrum, dN/dE , (normalized to the energy of the SM final state) for the given dark matter mass and SM final state [30]. N is the total number of neutrinos produced, derived from the neutrino energy distribution. Note that, for the energies we consider, typical RMS neutrino energies are $\sim 0.3m_b$. The scaling in eq. 3 can be understood by noting that both the muon range and the neutrino-nucleon cross section are proportional to neutrino energy at the energies we consider. Assuming the dark matter annihilates only to SM particles, a conservative estimate for neutrino production may be obtained by assuming that the annihilation to SM particles is dominated by $b\bar{b}$ production for $m_b < m_X < M_W$, by $\tau\bar{\tau}$ production for $M_W < m_X < m_t$, and by W, Z production for $m_X > m_t$ [32].

Super-K bounds the ν_μ -flux from dark matter annihilation in the Sun. Since the total annihilation rate is equal to the capture rate, this permits Super-K to bound the dark matter-nucleon scattering cross section using Eq. (2), assuming $\rho_X = 0.3 \text{ GeV cm}^{-3}$ and a Maxwellian velocity distribution with $\bar{v} \sim 220 \text{ km/s}$. In Fig. 1, we plot the published bounds from Super-K, as well as limits from other dark matter direct detection experiments and the regions of $(m_X, \sigma_{\text{SI}})$ parameter space favored by the DAMA signal given various astrophysical and detector uncertainties. As evident from Fig. 1, the published Super-K bounds (solid line) do not yet test the DAMA-favored regions. In the following section, however, we will see that consideration of the full Super-K event sample may provide marked improvements, and extend Super-K's sensitivity to low masses and the DAMA regions.

3. Projection of Super-K Sensitivity

The Super-K inner detector has a radius of 16.9 meters and a height of 36.2 meters. A muon event which is produced outside the inner detector, passes through and then leaves the inner detector is called a through-going muon. These events are subject to a cut requiring the muon to pass through at least 7 meters of the inner detector before exiting.

As shown in Fig. 1, Super-K currently reports dark matter bounds only down to $m_X = 18 \text{ GeV}$. The reason is that more massive dark matter particles produce energetic neutrinos that convert to energetic muons. For heavy dark matter, these muons are energetic enough that they pass all the way through the detector, thus providing maximal directional information, which can be used to distinguish these neutrinos from those that arise from atmospheric background. For dark matter above 18 GeV, the authors of Ref. [33] estimate that more than 90% of the upward-going muons will be

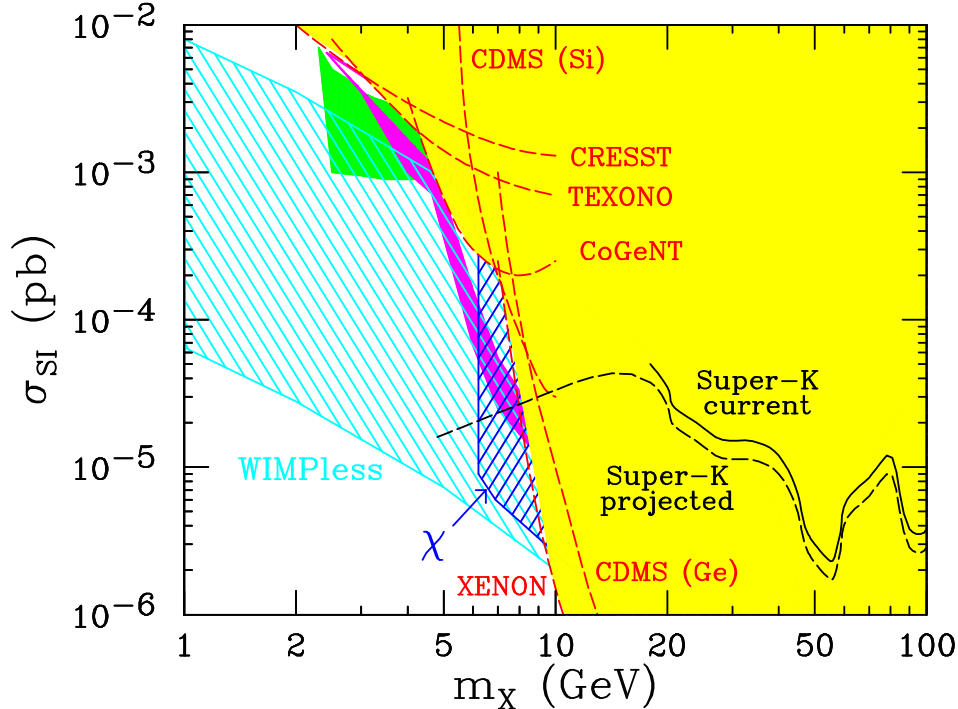


Figure 1. Direct detection cross sections for spin-independent X -nucleon scattering as a function of dark matter mass m_X . The black solid line is the published Super-K exclusion limit [33], and the black dashed line is our projection of future Super-K sensitivity. The magenta shaded region is DAMA-favored given channeling and no streams [13], and the medium green shaded region is DAMA-favored at 3σ given streams but no channeling [10]. The light yellow shaded region is excluded by the direct detection experiments indicated. The dark blue diagonal shaded (upper right to lower left) region is the prediction for the neutralino models considered in Ref. [19] and the light blue diagonal shaded region (upper left to lower right) region is the parameter space of WIMPless models with connector quark mass $m_Y = 400$ GeV and $0.3 < \lambda_b < 1.0$. Other limits come from the Baksan and MACRO experiments [17, 18, 33], though they are not as sensitive as Super-K.

through-going. However, one could study dark matter at lower masses by using stopping, partially contained, or fully contained muons, that is, upward-going muons that stop within the detector, begin within the detector, or both.

To determine rough projected bounds one may obtain from these event topologies, we adopt the following strategy. We begin by conservatively assuming that the measured neutrino spectrum at low energies matches the predicted atmospheric background. In any given bin with N neutrino events, the bound on the number of neutrinos from dark matter annihilation is then \sqrt{N} . This implies a bound on the dark matter annihilation rate to neutrinos, which, for a conservative choice of $\xi(m_X)$, yields a bound on the capture rate and therefore a bound on σ/m_X . To include experimental acceptances and efficiencies, we scale our results to the published limits at $m_X = 18$ GeV, assuming these effects do not vary greatly in extrapolating down to the 5 – 10 GeV range of interest.

The annihilation of dark matter particles X produces neutrinos with typical energies

between $1/3$ and $1/2$ of m_X . The Sun is effectively a point source of neutrinos. The directions of the observed muons, however, lie in a cone around the direction to the Sun, with rms half-angle of approximately[‡] $\theta = 20^\circ \sqrt{10 \text{ GeV}/E_\nu}$ [35]. In Ref. [33], bounds on dark matter with $m_X = 18 \text{ GeV}$ were set using neutrinos with energies $E_\nu \sim 6 - 9 \text{ GeV}$. The event sample used consisted of 81 upward through-going muons within a 22° angle of the Sun collected from 1679 live days.

To extrapolate to the masses $m_X \sim 5 - 10 \text{ GeV}$ of interest, we must consider neutrinos with energies between 2-4 GeV. From Ref. [36], one can see that at these energies, the detected events are dominantly fully-contained events, and so we use this event topology. The expected number of fully-contained events from all directions is given in Ref. [36] in bins with width 1 GeV. To determine the number of relevance to us, we restrict these events to those within the required cone around the Sun. The number of events is then

$$N_{\text{solar}} = N \frac{1 - \cos \theta}{2}, \quad (4)$$

where N is the total number of fully-contained events expected in the $2 - 4 \text{ GeV}$ energy range and θ is the cone opening angle appropriate for that range. We find $N = 168$ fully contained events per 1000 live days.

We then convert this limit on event rate to a limit on the neutrino flux by dividing by the effective cross section for the Super-K experiment in the relevant energy range. The effective cross-section for Super-K to neutrinos in a particular energy range is an exclusive cross-section to a particular sample of muon events (for example, throughgoing or fully contained) which are observed at Super-K. It is defined as the the rate of Super-K muon events within that sample and energy range divided by the atmospheric flux of neutrinos over that energy range. The effective cross-section can be estimated from Ref. [36] by dividing the estimated rate of events by the predicted atmospheric flux, integrated over the relevant range of energies. For fully contained events with neutrino energies between 2 and 4 GeV, we find that the effective cross section[§] is $\sim 2.1 \times 10^{-8} \text{ m}^2$. For upward through-going events with neutrino energies $\sim 8 \text{ GeV}$, the effective cross-section is $\sim 1.7 \times 10^{-8} \text{ m}^2$.

Assuming that the neutrino events are detected primarily in either the fully-contained ($2 - 4 \text{ GeV}$) or through-going sample, we can then set the following 2σ limits on the time-integrated neutrino flux due to dark matter annihilation:

$$\begin{aligned} \Phi_{\text{FC}}^{\text{max}} &= \frac{2\sqrt{N_{\text{FC}}}}{2.1 \times 10^{-8} \text{ m}^2} \sim 1.6 \times 10^9 \text{ m}^{-2} \sqrt{\frac{N_{\text{days}}}{1679}} \\ \Phi_{\text{TG}}^{\text{max}} &= \frac{2\sqrt{N_{\text{TG}}}}{1.7 \times 10^{-8} \text{ m}^2} \sim 1.0 \times 10^9 \text{ m}^{-2} \sqrt{\frac{N_{\text{days}}}{1679}}, \end{aligned} \quad (5)$$

[‡] This approximation is a rough estimate based on kinematics, but will be sufficient for our purposes.

[§] One can verify this by computing the neutrino- nucleon scattering cross-section and multiplying by the number of nucleons in the inner detector. The cross-section depends on the first moment of the neutrino spectrum, $\langle Nz \rangle$, which can be estimated from [32]. This calculation confirms the estimate from [36].

where $N_{\text{FC}} = 168 (N_{\text{days}}/1000)$ and $N_{\text{TG}} = 81 (N_{\text{days}}/1679)$ are the number of fully-contained and through-going events within the angle and energy ranges, respectively, scaled to N_{days} live days.

The ratio of these flux limits obtained from the fully-contained and through-going samples are then equal to the ratio of σ/m_X in the $5 - 10$ GeV regime to the same quantity at 18 GeV. We find

$$\frac{1.6 \times 10^9 \text{ m}^{-2}}{1.0 \times 10^9 \text{ m}^{-2}} \sim \left(\frac{\sigma_{5-10}}{m_{5-10}} \right) \left(\frac{\sigma_{18}}{18 \text{ GeV}} \right)^{-1}, \quad (6)$$

where σ_{5-10} is the Super-K bound on the dark matter nucleon cross-section for a dark matter particle with mass in the range $5 - 10$ GeV, and σ_{18} is the bound for a dark matter particle with mass 18 GeV. In Fig. 1 this projected Super-K bound is plotted, assuming 3000 live days of the SK I-III run.

We can check this projection by computing the bound on the annihilation rate to neutrinos, and comparing it to the capture rate. Given the expression for $\Phi_{\text{FC}}^{\text{max}}$ evaluated over 3000 live days and the distance from the sun to the earth, one finds an upper bound on the annihilation rate to neutrinos given by $\Gamma_{XX \rightarrow \nu_\mu \nu_\mu} < 2.3 \times 10^{24}$ events/s. Approximating $\Gamma_{XX \rightarrow \nu_\mu \nu_\mu} \sim \Gamma_{\text{total}} = \frac{1}{2}C$, we then find $\frac{\sigma}{m_X} < 6 \times 10^{-6} \frac{\text{pb}}{\text{GeV}}$. The resulting approximate bounds are within a factor of two of those plotted in Fig. 1.

Note that, unlike direct detection experiments, this bound does not become much worse at lower energies. Indeed, Super-K may beat other experiments at these energies, and the bound improves significantly with time, in contrast to direct detection experiments, where the bounds at low mass are essentially limited by energy thresholds. Moreover, it is important to note that any individual model will have its own specific neutrino energy spectrum, and analysis with this spectrum in mind will enhance the sensitivity of Super-K to that model.

We expect that the projected sensitivities derived here are conservative for several reasons. First, events from the Earth's core may be included. In fact, there may be hydrogen in the Earth's core [37], leading to an enhancement of event rates at the low masses of interest here. Second, for the various data sets and employing a single joint fit, one can use the expected angular distribution of muon and electron products of the solar and Earth neutrinos from dark matter annihilations, instead of a simple cone which includes all (and too much background). This can be done as a function of energy for the contained events (stopping and through-going muons being all binned together). In addition, using off-source fake cones can provide background checks free of Monte-Carlo systematic error concerns. Of course, if any hint of excess exists, one can start to test for such things as ν_μ/ν_e ratio and the particle to anti-particle ratio (via stopped muon decays and again perhaps employing on-source to off-source systematic canceling tests). Note however that, since for dark matter masses in the few GeV range the angular size of the capture region in the Earth will be large, one may have to worry about confusing any terrestrial annihilations with atmospheric neutrino oscillations.

4. Prospects for Various Dark Matter Candidates

We now consider specific examples of theoretical models that have been proposed to explain the DAMA result. We present these both to highlight various theoretical assumptions that have been made in the previous discussion, and to provide concrete examples of what future super-K analyses may tell us.

We first consider neutralino dark matter in supersymmetric models. Although neutralinos typically have larger masses and lower cross sections than required to explain the DAMA signal, special choices of supersymmetry parameters may yield values in the DAMA-favored region. Such models have been discussed in Ref. [19]. In particular, gaugino masses are not unified in these models, so that neutralinos with masses below 10 GeV are not in conflict with chargino masses bounds.

The region of the $(m_X, \sigma_{\text{SI}})$ plane spanned by the models of Ref. [19] that do not violate known constraints is given in Fig. 1. The range in σ_{SI} results largely from nuclear uncertainties. We see that if Super-K's limits can be extended to lower mass and our conservative projection improved as discussed above, Super-K could find evidence for models in this class. We note, however, that these models are required only to have relic densities that do not overclose the Universe; many of them have $\rho < 0.3 \text{ GeV cm}^{-3}$. For these models, Super-K's bound on the cross section will be less sensitive than reported under the assumption $\rho = 0.3 \text{ GeV cm}^{-3}$ (see Eq. (2)).

WIMPless dark matter provides an alternative explanation of the DAMA/LIBRA signal [12]. These candidates are hidden sector particles that naturally have the correct relic density [21]. In these models, the dark matter particle X couples to SM quarks via exchange of a connector particle Y that is similar to a 4th generation quark. The Lagrangian for this interaction is

$$\mathcal{L} = \lambda_f X \bar{Y}_L f_L + \lambda_f X \bar{Y}_R f_R . \quad (7)$$

The Yukawa couplings λ_f are model-dependent, and it is assumed that only the coupling to 3rd generation quarks is significant, while the others are Cabibbo-suppressed.|| In this case, one finds that the dominant nuclear coupling of WIMPless dark matter is to gluons via a loop of b -quarks (t -quark loops are suppressed by m_t). The X -nucleus cross section is then given by [12]

$$\sigma_{\text{SI}} = \frac{1}{4\pi} \frac{m_N^2}{(m_N + m_X)^2} \left[\sum_q \frac{\lambda_b^2}{m_Y - m_X} [Z B_b^p + (A - Z) B_b^n] \right]^2 , \quad (8)$$

where Z and A are the atomic number and mass of the target nucleus N , and $B_b^{p,n} = (2/27) m_p f_g^{p,n} / m_b$, where $f_g^{p,n} \simeq 0.8$ [38, 39].

In Fig. 1, the range in the $(m_X, \sigma_{\text{SI}})$ parameter space for WIMPless models with $m_Y = 400 \text{ GeV}$ and $0.3 < \lambda_b < 1.0$ is also given. We see that these models span a large range in the $(m_X, \sigma_{\text{SI}})$ plane, and may overlap all parts of the DAMA-favored region. In this case, since dark matter annihilation to SM particles proceeds only through the

|| This is a reasonable assumption and is consistent with small observed flavor-changing neutral currents.

$b\bar{b}$ channel, the conservative Super-K estimate for $\xi(m_X)$, defined in Eq. (3), is largely correct. We see that Super-K’s projected sensitivity may be sufficient to discover a signal that corroborates DAMA’s.

WIMPless models illustrate an important caveat to the analysis above, however. In WIMPless models, dark matter may also annihilate to hidden sector particles, which, of course, do not produce neutrinos detectable at Super-K. If there are hidden decay channels, then the annihilation rate to SM particles is

$$\Gamma_{SM} = B(X\bar{X} \rightarrow SM)\Gamma_{tot} = B(X\bar{X} \rightarrow SM)C, \quad (9)$$

and one should divide the Super-K limit by $B(X\bar{X} \rightarrow SM)$ to obtain the Super-K bound in the presence of hidden decay channels.

The cross section for annihilation to hidden sector particles cannot be arbitrarily large, however, if the thermal relic density is to remain significant. In this WIMPless model, for $\lambda_b = 0.5$, the cross-section for annihilation to SM particles is already $(\sigma v)_{SM} \sim 7$ pb. WIMPless dark matter also annihilates to hidden sector particles through hidden gauge interactions. In contrast to neutralinos and other visible sector dark matter candidates, however, for WIMPless dark matter the precise relation between this annihilation cross section and the relic density depends on some model-dependent factors, such as the number of relativistic degrees of freedom in the hidden sector and the ratio of hidden and visible sector temperatures [22]. For reasonable values of these parameters, the models plotted in Fig. 1 can have a relic density that is 10 – 100% of the observed density of dark matter. For the lower densities in this range, Super-K’s sensitivity will be proportionally worse, according to Eq. (2). In any case, if Super-K’s reach can extend to lower mass, it could reasonably find evidence for (or place constraints on) these models.

Finally, we consider mirror dark matter, which has also been advanced as a DAMA-explaining possibility [23]. These models require a slightly more detailed analysis. In this case, the dark matter candidate is a hidden sector particle with mass $\sim 10 – 30$ GeV that interacts with the SM through kinetic mixing with the photon. Because scattering occurs through exchange of a massless particle, one finds here that $\sigma \propto E_R^{-2}$, where E_R is the recoil energy. This is why mirror dark matter can be seen at DAMA while evading bounds from other direct detection experiments — the cross section is highest for scattering at low recoil energies, which are below the threshold of other other experiments, but above the 2 keV threshold of DAMA.

To understand the limits Super-K can place on this type of model, we must essentially find the “threshold” of the Sun, thought of as a direct detection device. The Sun only captures particles that lose an energy E_0 during elastic scattering, where E_0 is the kinetic energy of the particle when it was far from the Sun. E_0 is essentially the threshold recoil energy required for dark matter capture. For a halo velocity ~ 220 km/s and a mass ~ 20 GeV, we find $E_0 \sim 5$ keV. The solar capture rate is unaffected (to first approximation) by scattering at lower recoil energies; essentially, for the purposes of a

mirror matter study, Super-K is a high-threshold experiment¶. Indeed, the threshold is higher than that of XENON10 (4.5 keV). In the relevant mass range, a mirror matter candidate that could explain the DAMA signal cannot be detected by XENON10 [23]. Since XENON10 has higher sensitivity than Super-K in this mass region, and the cross-section relevant for Super-K is slightly smaller than that for XENON10, one expects that Super-K also will not be able to bound mirror matter. We note, however, that models with $m \sim 10$ GeV may be constrained by Super-K.

5. Summary

The DAMA/LIBRA signal is currently of great interest, and alternative methods for corroborating or excluding a dark matter interpretation are desired. In this study, we have shown that the preferred DAMA region implies that Super-K, through its search for dark matter annihilation to neutrinos, has promising prospects for testing DAMA.

We have given a conservative estimate of the projected sensitivity of Super-K. By using fully contained events, we expect that current super-K bounds may be extended to dark matter masses of 5 to 10 GeV. In the region of most interest for the DAMA result with $m_X \sim 5 - 10$ GeV, the neutralino models of Ref. [19] and WIMPless models can potentially be tested, provided the sensitivities expected at this low mass range are actually realized. For mirror matter, however, the mass range of interest is 10 – 30 GeV, and it is unlikely that Super-K can place limits on this model.

We thus have the intriguing prospect that the direct detection result of DAMA/LIBRA could be sharply tested by an indirect detection experiment in the very near future.

Acknowledgments

We are grateful to Huitzu Tu, Hai-Bo Yu and, especially, Hank Sobel for discussions. This work was supported by NSF grants PHY-0239817, PHY-0314712, PHY-0551164 and PHY-0653656, DOE grant DE-FG02-04ER41291, and the Alfred P. Sloan Foundation. Support for this work for LES was provided by NASA through Hubble Fellowship grant HF-01225.01 awarded by the Space Telescope Science Institute, which is operated by the Association of Universities for Research in Astronomy, Inc., for NASA, under contract NAS 5-26555. JK is grateful to CERN and the organizers of Strings '08, where part of this work was done, for their hospitality.

¶ Note that this is in contrast to Super-K probes of WIMPs, which Super-K can study at low mass. This difference arises because, with mirror matter, the issue is the scaling of the cross-section with recoil energy. The suppression of the cross-section at high recoil energy does not typically occur with WIMP models.

- [1] R. Bernabei *et al.*, [DAMA Collaboration], arXiv:0804.2741 [astro-ph]; Riv. Nuovo Cim. **26N1**, 1 (2003) [arXiv:astro-ph/0307403]; Int. J. Mod. Phys. D **13**, 2127 (2004) [arXiv:astro-ph/0501412].
- [2] A. K. Drukier, K. Freese and D. N. Spergel, Phys. Rev. D **33**, 3495 (1986); K. Freese, J. A. Frieman and A. Gould, Phys. Rev. D **37**, 3388 (1988).
- [3] G. Angloher *et al.*, Astropart. Phys. **18**, 43 (2002).
- [4] D. S. Akerib *et al.*, [CDMS Collaboration], Phys. Rev. Lett. **96**, 011302 (2006) [arXiv:astro-ph/0509259]; Z. Ahmed *et al.*, [CDMS Collaboration], arXiv:0802.3530 [astro-ph].
- [5] J. Angle *et al.*, [XENON Collaboration], Phys. Rev. Lett. **100**, 021303 (2008) [arXiv:0706.0039 [astro-ph]].
- [6] S. T. Lin *et al.*, [TEXONO Collaboration], arXiv:0712.1645 [hep-ex].
- [7] F. T. Avignone, P. S. Barbeau and J. I. Collar, arXiv:0806.1341 [hep-ex].
- [8] C. E. Aalseth *et al.*, arXiv:0807.0879 [astro-ph].
- [9] See, *e.g.*, M. Brhlik and L. Roszkowski, Phys. Lett. B **464**, 303 (1999) [arXiv:hep-ph/9903468]; P. Belli, R. Bernabei, A. Bottino, F. Donato, N. Fornengo, D. Prosperi and S. Scopel, Phys. Rev. D **61**, 023512 (2000) [arXiv:hep-ph/9903501].
- [10] P. Gondolo and G. Gelmini, Phys. Rev. D **71**, 123520 (2005) [arXiv:hep-ph/0504010].
- [11] R. Bernabei *et al.*, Eur. Phys. J. C **53**, 205 (2008) [arXiv:0710.0288 [astro-ph]].
- [12] J. L. Feng, J. Kumar and L. E. Strigari, arXiv:0806.3746 [hep-ph].
- [13] F. Petriello and K. M. Zurek, arXiv:0806.3989 [hep-ph].
- [14] S. Chang, A. Pierce and N. Weiner, arXiv:0808.0196 [hep-ph].
- [15] M. Fairbairn and T. Schwetz, arXiv:0808.0704 [hep-ph].
- [16] C. Savage, G. Gelmini, P. Gondolo and K. Freese, arXiv:0808.3607 [astro-ph].
- [17] T. Montaruli [MACRO Collaboration], arXiv:hep-ex/9905020.
- [18] C. de los Heros, *et al.*, arXiv:astro-ph/0701333.
- [19] A. Bottino, F. Donato, N. Fornengo and S. Scopel, Phys. Rev. D **68**, 043506 (2003) [arXiv:hep-ph/0304080]; Phys. Rev. D **77**, 015002 (2008) [arXiv:0710.0553 [hep-ph]]; arXiv:0806.4099 [hep-ph].
- [20] D. Tucker-Smith and N. Weiner, Phys. Rev. D **64**, 043502 (2001) [arXiv:hep-ph/0101138]; Phys. Rev. D **72**, 063509 (2005) [arXiv:hep-ph/0402065].
- [21] J. L. Feng and J. Kumar, arXiv:0803.4196 [hep-ph].
- [22] J. L. Feng, H. Tu and H. B. Yu, arXiv:0808.2318 [hep-ph].
- [23] R. Foot, arXiv:0804.4518 [hep-ph].
- [24] M. Y. Khlopov and C. Kouvaris, arXiv:0806.1191 [astro-ph].
- [25] S. Andreas, T. Hambye and M. H. G. Tytgat, arXiv:0808.0255 [hep-ph].
- [26] E. Dudas, S. Lavignac and J. Parmentier, arXiv:0808.0562 [hep-ph].
- [27] D. Hooper, F. Petriello, K. M. Zurek and M. Kamionkowski, arXiv:0808.2464 [hep-ph].
- [28] A. Gould, Astrophys. J. **321**, 571 (1987).
- [29] K. Griest and D. Seckel, Nucl. Phys. B **283**, 681 (1987) [Erratum-ibid. B **296**, 1034 (1988)].
- [30] M. Kamionkowski, K. Griest, G. Jungman and B. Sadoulet, Phys. Rev. Lett. **74**, 5174 (1995) [arXiv:hep-ph/9412213].
- [31] A. Gould, Astrophys. J. **321**, 560 (1987).
- [32] G. Jungman and M. Kamionkowski, Phys. Rev. D **51**, 328 (1995) [arXiv:hep-ph/9407351].
- [33] S. Desai *et al.* [Super-Kamiokande Collaboration], Phys. Rev. D **70**, 083523 (2004) [Erratum-ibid. D **70**, 109901 (2004)] [arXiv:hep-ex/0404025].
- [34] D. N. Spergel and W. H. Press, Astrophys. J. **294**, 663 (1985).
- [35] G. Jungman, M. Kamionkowski and K. Griest, Phys. Rept. **267**, 195 (1996) [arXiv:hep-ph/9506380].
- [36] Y. Ashie *et al.* [Super-Kamiokande Collaboration], Phys. Rev. D **71**, 112005 (2005) [arXiv:hep-ex/0501064].
- [37] Q. Williams and R. Hemley, Annu. Rev. Earth Planet Sci. **29**, 365 (2001).
- [38] H. Y. Cheng, Phys. Lett. B **219**, 347 (1989).

[39] J. R. Ellis, J. L. Feng, A. Ferstl, K. T. Matchev and K. A. Olive, Eur. Phys. J. C **24**, 311 (2002) [arXiv:astro-ph/0110225].